Addressing matrix effects for 193 nm excimer LA-ICP-MS analyses of Fe-rich sulfides and a new predictive model

Steenstra, E. S.; Berndt, J.; Klemme, S.; Van Westrenen, W.; Bullock, E. S.; Shahar, A.

published in
Journal of Analytical Atomic Spectrometry
2020

DOI (link to publisher)
10.1039/c9ja00391f

document version
Publisher's PDF, also known as Version of record

JAAS

ROYAL SOCIETY OF CHEMISTRY

PAPER

View Article Online
View Journal | View Issue

Cite this: *J. Anal. At. Spectrom.*, 2020, **35**, 498

Addressing matrix effects for 193 nm excimer LA-ICP-MS analyses of Fe-rich sulfides and a new predictive model†

E. S. Steenstra, *[abc] J. Berndt,[b] S. Klemme,[b] W. van Westrenen,[c] E. S. Bullock [a] and A. Shahar[a]

Laser-ablation inductively coupled plasma mass spectrometry (LA-ICP-MS) is one of the most popular techniques for determining trace element concentrations in sulfides. Due to the lack of matrix-matched standards, standardization of sulfide analyses are usually based on silicate glass calibrant materials. Matrix effects during ns-LA-ICP-MS analyses of Fe-rich sulfides were quantified for many trace elements by comparison of elemental concentrations obtained by LA-ICP-MS and electron microprobe (EPMA) for many synthetic sulfides. The data was used to obtain the fractionation indices (F_i, the ratio between the EPMA- and LA-ICP-MS-determined concentrations of element i) for many elements while considering Fe, Cu and Ni as internal standards. The results show that significant (>15% RD) matrix effects arise during ns-LA-ICP-MS analyses of Ti, Zn, Ge, Se, Mo, Cd, In, Sb, Te, Pb, Bi in sulfides when using Fe as the internal standard. The use of Ni as an internal standard yields on average higher F_i values for most elements, resulting in more pronounced matrix effects for refractory elements and less so for volatile elements, relative to Fe. The use of Cu as an internal standard yields overall more significant matrix effects for volatile elements (*i.e.*, lower F_i values). The F_i values for most elements remain constant with increasing concentrations, and matrix correction factors for these elements can therefore be applied across the ppm to wt% range. In agreement with previous observations for Fe-rich metals and silicate glasses, the magnitudes of the matrix effects for the various elements are strongly correlated with elemental volatility. This correlation was used to obtain a predictive model for describing F_i for Fe-rich sulfides. The results were used to assess the effects of matrix effects on calculated sulfide liquid–silicate melt partition coefficients derived from experiments. Matrix effects arising through the use of non-matrix-matched standards will result in significant discrepancies between measured and true partition coefficients, the extent mainly depending of the volatility of the element considered. Corrections on ns-LA-ICP-MS derived element concentrations therefore need to be performed to obtain true abundances in the absence of matrix-matched standards.

Received 15th November 2019
Accepted 8th January 2020

DOI: 10.1039/c9ja00391f

rsc.li/jaas

1. Introduction

Laser-ablation inductively coupled plasma mass spectrometry (LA-ICP-MS) is a popular technique to quantify trace element abundances in sulfides that are relevant to many scientific fields, including archaeology,[1] planetary science,[2] the metallurgical industry[3] and terrestrial[4] and experimental geochemistry.[5,6] The ablation behavior of elements during LA-ICP-MS analyses of sulfides and other samples depends on a range of material properties. These properties include target surface reflectivity, optical absorption coefficient, thermal diffusivity and melting or boiling temperature and corresponding properties such as target surface temperature and amount of laser-induced vaporization.[7] It is well established that the relative contribution of these effects to elemental and isotopic fractionation during ns-LA-ICP-MS analysis can be strongly dependent on sample compositions or matrices, as demonstrated for Fe-based materials,[7–12] sulfides[13–15] and silicate glasses.[16]

Although some Fe-rich sulfide reference materials are available, several issues may exist with these materials. Sulfide reference materials are often heterogeneous with respect to major and minor element distributions[17] or they contain only a limited set of elements, predominantly the highly siderophile elements (HSE).[18–20] Some sulfide reference materials have different ablation characteristics relative to the sample of interest (in the case of pressed powder standards[17]) and/or many sulfide reference materials have been consumed or are

[a]*The Geophysical Laboratory, Carnegie Institution for Science, Washington D.C., USA. E-mail: esteenstra@carnegiescience.edu*

[b]*Institute of Mineralogy, University of Münster, Germany*

[c]*Vrije Universiteit Amsterdam, The Netherlands*

† Electronic supplementary information (ESI) available. See DOI: 10.1039/c9ja00391f

not available for use by other groups. The use of fs-based laser systems dramatically decreases matrix effects,[8] but these systems can be technically challenging relative to ns-based LA-ICP-MS systems and are more expensive to operate.[21,22] The use of silicate primary standards for calibrating quantitative analyses of sulfides therefore remains a popular approach,[5,6,23–25] but this approach could yield erroneous results if matrix effects are not taken into account.

To quantitatively assess the matrix effects in the latter approach, we extend our previous work for Fe-rich metal alloys[26] to Fe-rich sulfides and obtained a large set of fractionation indices (F_i values, defined as ratio between the EPMA- and LA-ICP-MS determined elemental concentrations) for many elements. New F_i values for sulfides were obtained by analysing experimentally synthesized Fe-rich sulfides with ns-LA-ICP-MS and electron microprobe (EPMA). The F_i values were calculated through quantitative comparison of the results of both techniques in conjunction with previously published data obtained using the same or similar LA-ICP-MS and EPMA setups.[6,27–30] The results were compared with previously derived F_i values for Fe-rich, S-poor metal alloys obtained using the same or a similar LA-ICP-MS setup.[26] The magnitude of matrix effects was independently assessed for three commonly used internal standards (Fe, Ni, Cu) and a new model was derived that allows for addressing the matrix effects arising through ns-LA-ICP-MS analyses of Fe-rich sulfides using non-matrix-matched standard materials.

2. Methods

2.1 Synthetic Fe-rich sulfides

Synthetic Fe-rich sulfides were obtained by mixing FeS metal powders with variable amounts (0.1 to 2 wt%; Alpha Aesar, >99.5% purity) of a variety of elements (V, Cr, Mn Co, Ni, Cu, Zn, Ge, As, Se, Mo, Cd, In, Sn, Sb, Te, W, Pb, Bi) under ethanol in an agate mortar for >30 minutes. Elements were clustered in subgroups to decrease the total doping levels of trace elements to the Fe–S matrix (Table S1†). Sulfide powders were combined with powdered silicate glasses in an approximate 4 : 1 ratio to further improve cohesion of the sulfides. The powders were loaded into graphite capsules (3.1 mm O.D.; 1.6 mm I.D., 4 mm long) with tightly fitting graphite lids that were machined from high-purity graphite rods. The samples were synthesized at high pressure (1 GPa) and 1883 K using a piston cylinder apparatus at the Vrije Universiteit Amsterdam.[6] After the experiments, the samples were embedded in epoxy resin and polished wet using various grades of SiC sandpaper and nano-diamond-doped lubricants. Fig. S.1† in the Appendix shows examples of typical run products.

2.2 EPMA analyses

Major and trace element compositions of the sulfides were obtained using JEOL JXA 8530F field emission electron microprobes at the Institute of Mineralogy, University of Münster, and the Geophysical Laboratory, Carnegie Institution for Science. Analyses were performed using a defocused beam (5–15 μm) because of the quench-induced heterogeneous nature of the sulfide liquids at smaller scales (Fig. S 1†). Measurement points were set in random lines and/or raster grids, depending on the available surface area of the analysed phases. Beam currents were 15–20 nA and an accelerating voltage of 15 kV. Dwell times were 10–30 s on peak and 5–15 s on each background. The use of a large number of spot analyses per sample (usually between 60–100 spots) was used to ensure a representative average chemical composition of each sulfide was obtained.

Standards used for sulfide analyses were diopside or anorthite for Ca, Fe metal or fayalite for Fe, Mn_2O or rhodonite for Mn, Zn–metal or willemite for Zn, PbS or Pb–Zn glass for Pb, InAs or GaAs for As, anorthite or hypersthene for Si, PbS or pyrite for S, $MgCr_2O_4$ or Cr_2O_3 for Cr, NiSe or NiO for Ni, NiSe or pure metal for Se, CdTe or pure metals for Cd and Te, InAs or pure metal for In, TiO_2 or pure metal for TiO_2, and only pure metal standards for V, Co, Cu, Ge, Sn, Sb, Mo, W and Bi. Calibrations were considered successful when the primary standard compositions were reproduced within 1% relative deviation. Data reduction was performed using the $\Phi(\rho Z)$ approach[31] or the ZAF correction, which corrects for the decrease in X-ray density due to the distance the X-rays have to travel through the specimen before they reach the detector. Steenstra *et al.*[26] confirmed the accuracy of our analytical approach using analyses of the NIST 610 reference glass. These measurements were made at the start of the analyses period of this study. In the latter study good agreement (*i.e.*, within 10% relative deviation) was observed between reference and measured values, despite the low concentrations of the various elements (500 ppm) and the use of a moderate beam current of 15 nA. We confirmed the latter findings by repeating these analyses at the end of the analysis period of the samples presented in this study (Appendix Section A.1 and Fig. S.2†). The NIST 616 glass was also measured to assess true zero counts for the elements of interest and to confirm the accuracy and precision of our analytical approach.

2.3 LA-ICP-MS analyses

Laser ablation inductively coupled plasma mass spectrometry (LA-ICP-MS) analyses of sulfides were performed using a 193 nm ArF excimer laser (Analyte G2, Photon Machines) at the University of Münster[26] in conjunction with a Thermo Element II or Thermo Element XR – ICP-MS (Table 1). The LA-ICP-MS analyses were performed using a repetition rate of 10 Hz and a laser fluence of ~3–4 J cm^{-2}. The analyses were performed using 50 or 65 μm spot sizes. The elemental analyses were performed with a Thermo Element II (runs ESS-35 to ESS-75) using the same conditions outlined in Steenstra *et al.*[26] or with a Thermo XR-ICP-MS (runs ESS-81 to ESS-89).

Thermo Element II analyses were performed using the following settings (see also Table 1). The forward power was 1300 W and the reflected power <2 W. The gas flow rates were 1.2 L min^{-1} for He (the carrier gas of ablated material), 0.9 L min^{-1} and 1.1 L min^{-1} for the Ar-auxiliary and sample gas, respectively. Cooling gas flow rate was set to 16 L min^{-1}. Prior to

Table 1 Details of analytical set-up and settings

Laser ablation system	
Make, model, type	Photon machines, analyte G2, excimer laser
Ablation cell	HelEx 2-volume cell
Fluence	3–4 J cm^{-2}
Repetition rate	10 Hz
Ablation duration	40 s
Spot diameter	50/65 μm
Sampling mode/pattern	Static
Carrier gas	He in the cell, Ar sampling and cooling gas
Cell carrier gas flow	0.7 L min^{-1} for MFC1, 0.3 L min^{-1} for MFC2
ICP-MS instrument	
Make, model, type	ThermoFisher element 2/XR single collector ICP-MS
Sample introduction	Ablation aerosol
RF power	1300 W
Sample-, auxiliary-, and cooling gas flow	1.2 L min^{-1}, 0.9 L min^{-1}, 16 L min^{-1}
Number of runs	28
Background time	20 s
Data processing	
Calibration strategy	NIST 612 as primary reference material
Internal standards	^{56}Fe (sulfide), ^{63}Cu (sulfide), ^{60}Ni (sulfide), ^{29}Si (silicate glass)
Data processing software	Glitter®[40]
Quality control materials	BIR-1G, BCR-2G, NIST 610

analysis, the system was tuned on a NIST 612 glass measuring ^{139}La, ^{232}Th and $^{232}Th^{16}O$ to obtain stable signals and high sensitivity, as well as low oxide rates ($^{232}Th^{16}O/^{232}Th$ <0.1%) during ablation. For the LA-ICP-MS analyses performed with the Thermo XR-ICP-MS, Ar-auxiliary and sample gas were 0.75 L min^{-1} and 0.805 L min^{-1}, respectively. Cooling gas was also set to 16 L min^{-1} while the He flow rate was set to 0.9 L min^{-1}. The following isotopes were measured: ^{24}Mg, ^{29}Si, ^{43}Ca, ^{51}V, ^{53}Cr, ^{55}Mn, ^{56}Fe, ^{59}Co, ^{60}Ni, ^{61}Ni, ^{63}Cu, ^{66}Zn, ^{69}Ga, ^{73}Ge, ^{75}As, ^{82}Se, ^{95}Mo, ^{111}Cd, ^{115}In, ^{118}Sn, ^{121}Sb, ^{125}Te, ^{182}W, ^{208}Pb and ^{209}Bi.

The NIST 612 reference glass was used as a calibrant for all sulfide analyses. The USGS BIR-1G, BCR-2G and/or NIST 610 silicate reference materials were measured every ~20–25 LA-ICP-MS spots to assess accuracy and precision. No memory effects (*i.e.*, long-term build-up) were observed for any of the elements. All data were reduced using the GLITTER software package, using Si as the internal standard for analyses of USGS silicate glasses reference materials or Fe, Ni or Cu for the synthetic sulfides. The use of various internal standards for the same set of analyses allowed for optimization of the internal standard choice and for assessment of the effects of internal standard choice on derived matrix effects of LA-ICP-MS analyses of sulfides. In Appendix Section A.2† quantitative comparisons are provided between the preferred/previously reported major and trace element concentrations in the NIST 610, BIR-1G and BHVO-2G glasses and those measured in this study using the LA-ICP-MS approaches outlined above. As in our previous study,[26] good agreement is observed between the preferred values from the GeoRem dataset and the measured concentrations (*i.e.*, <10% relative deviation; Fig. S.3†).

3. Results

3.1 Fractionation indices for LA-ICP-MS analyses of sulfides

The left panels in Fig. 1–4 show the measured concentrations of the various elements in the sulfides measured by EPMA and LA-ICP-MS, while using Fe as the internal standard for LA-ICP-MS data reduction. In conjunction with previously published datasets of sulfide compositions that were obtained using similar EPMA and LA-ICP-MS techniques and settings,[6,27–30] the fractionation indices appropiate for sulfides for the different elements were quantified using eqn (1):[26]

$$F_i = \frac{\text{reference concentration by weight of element i in sulfide(EPMA)}}{\text{concentration by weight of element i in sulfide(LA-ICP-MS)}} \quad (1)$$

The F_i values were derived using linear regression fits to EPMA and LA-ICP-MS measurements for each element obtained for each synthetic sulfide. The latter values are indicative of the relative differences between both approaches – a lower F_i value implies preferential ablation of that specific element during LA-ICP-MS analysis and *vice versa*.

Table 2 lists the calculated F_i values. The EPMA and LA-ICP-MS-measured concentrations of the lesser-volatile and transitional elements (Mg, Mn, Co, Ni, Cu, As) are very similar, reflected by their F_i values that approximate unity (Table 2 and Fig. 5). As observed for Fe-rich metal alloys,[14,26,32] it is found that the concentrations of volatile elements (Zn, Ge, Cd, In, Sb, Te, Pb, Bi) are overestimated by LA-ICP-MS, relative to EPMA, and that many refractory elements (Cr, Ti, Mo, Pt) are underestimated. A notable exception is Se, which shows a significant higher but consistent F_i value, relative to elements with similar volatilities. Selenium does not show such behavior in S-poor metals.[26] The reason for this anomalous behavior is unclear, but it is most likely due to significant non-ideal volatility behavior of Se in the plasma. The results also show that F_i values for most elements remain constant at up to several wt%, consistent with previous results for Fe-rich metal alloys.[26] The F_i values of Zn, Cu and Se are not constant with concentration and are strongly increased at concentrations exceeding 1, 2 and 0.5 wt%, respectively (Fig. 2, 3).

The F_i values for Fe-rich sulfides obtained in this study are shown as a function of their volatility (approximated here using their 50% condensation temperatures[16,26,33,34]) in Fig. 5, in conjunction with previously derived F_i values for S-poor metal alloys[8,26] and Fe-rich sulfides.[13,35] As for Fe-rich metals[26] and silicate glasses,[16] a strong correlation is observed between F_i values and their 50% condensation temperatures (Fig. 5), that can be described by the following equation:

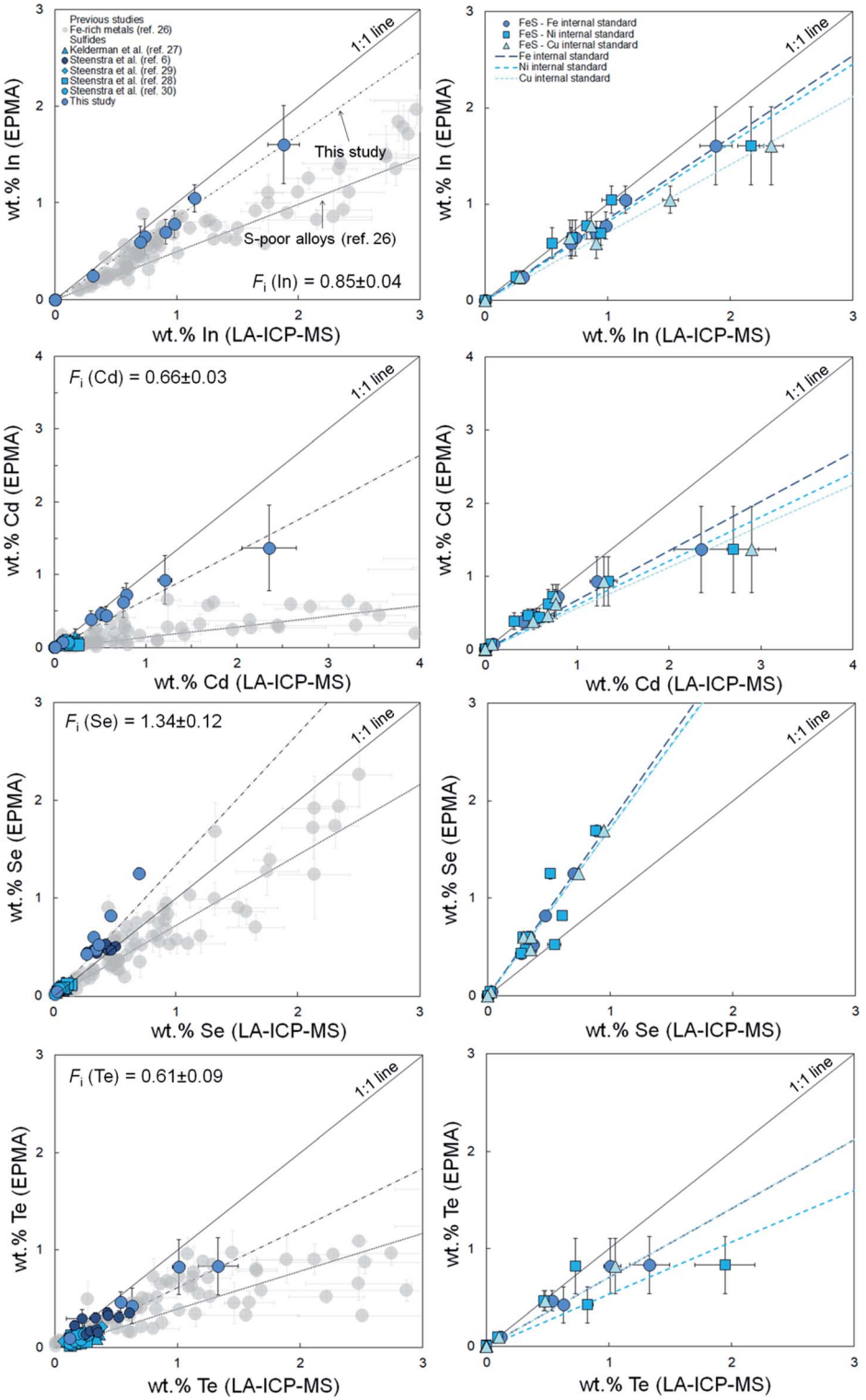

Fig. 1 Comparison between measured concentrations (%, in mass) of In, Cd, Se and Te using LA-ICP-MS and EPMA for Fe-rich sulfides. Left panels show the LA-ICP-MS concentrations of compiled and new sulfide analyses obtained using Fe as the internal standard. The coarse dashed lines in left panels represent fits to Fe-rich sulfides obtained in this study (Table 2). Left panels include previously obtained measurements for S-poor Fe-rich metal alloys;[26] fine dashed lines in left panels represent derived F_i trends for the latter data.[26] Right panels show a comparison of the measured concentrations by LA-ICP-MS (this study only) using Fe, Ni or Cu as the internal standard. Solid lines in left and right panels are 1 : 1 identity lines plotted for reference. Horizontal and vertical error bars in left and right panels represent 2 standard errors.

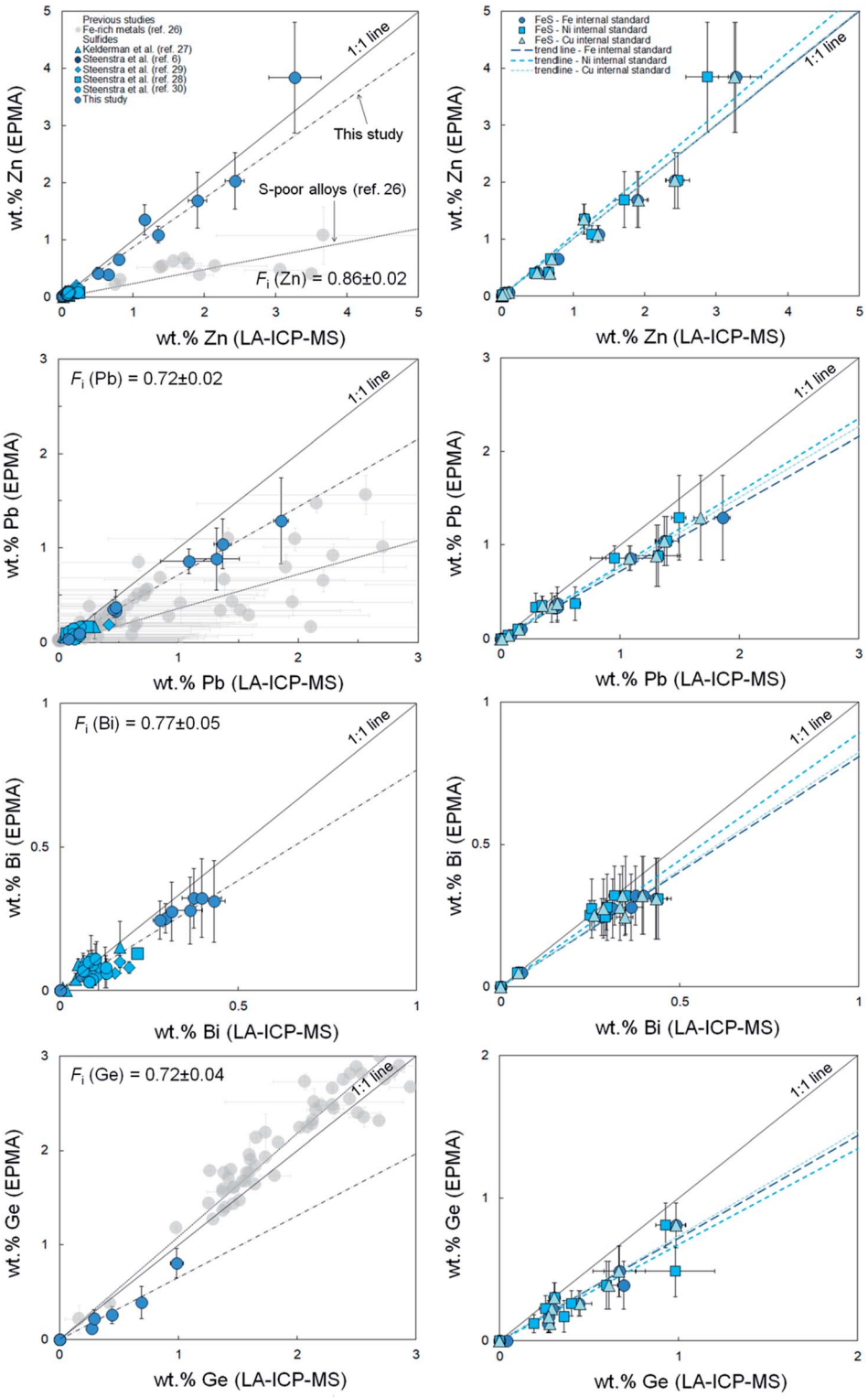

Fig. 2 Comparison between measured concentrations (%, in mass) of Zn, Pb, Bi and Ge using LA-ICP-MS and EPMA for Fe-rich sulfides. See Fig. 1 caption for additional details.

$$F_i = 0.000534 \pm 0.000077 \times 50\%\ T\ (\mathrm{K}) + 0.357 \pm 0.086\ (R^2 = 0.75) \quad (2)$$

The strong correlation between the magnitude of matrix effects and elemental volatility is consistent with previous hypotheses that attribute the matrix effects to volatility-related fractionation processes during and/or following ablation, as has been previously proposed for Fe-based samples,[8,26] sulfides[13,35] and silicate glasses.[16] Eqn (2) was also used to calculate the F_i values for elements for which at present no

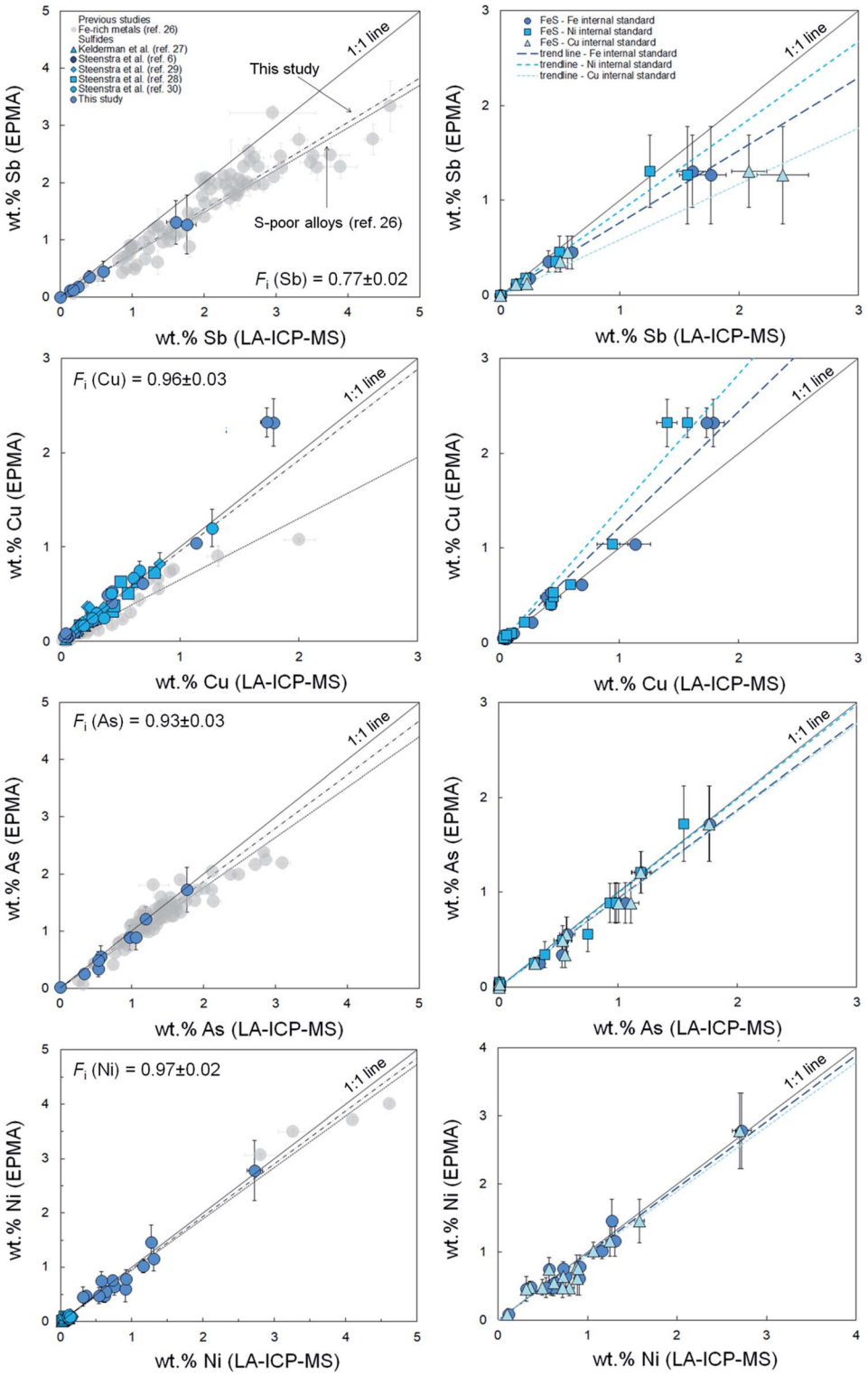

Fig. 3 Comparison between measured concentrations (%, in mass) of Sb, Cu, As and Ni using LA-ICP-MS and EPMA for Fe-rich sulfides. See Fig. 1 caption for additional details.

EPMA and/or LA-ICP-MS data are available or for elements for which EPMA concentrations cannot be obtained due to their low concentrations in sulfides (Si, P, S, K, V, Ga, Nb, Sn, Ta, W, Tl, Table 2).

3.2 Effect of internal standard choice on fractionation indices

To assess the potential effects of internal standard choice on matrix effects, we compared the F_i values, derived using Fe as

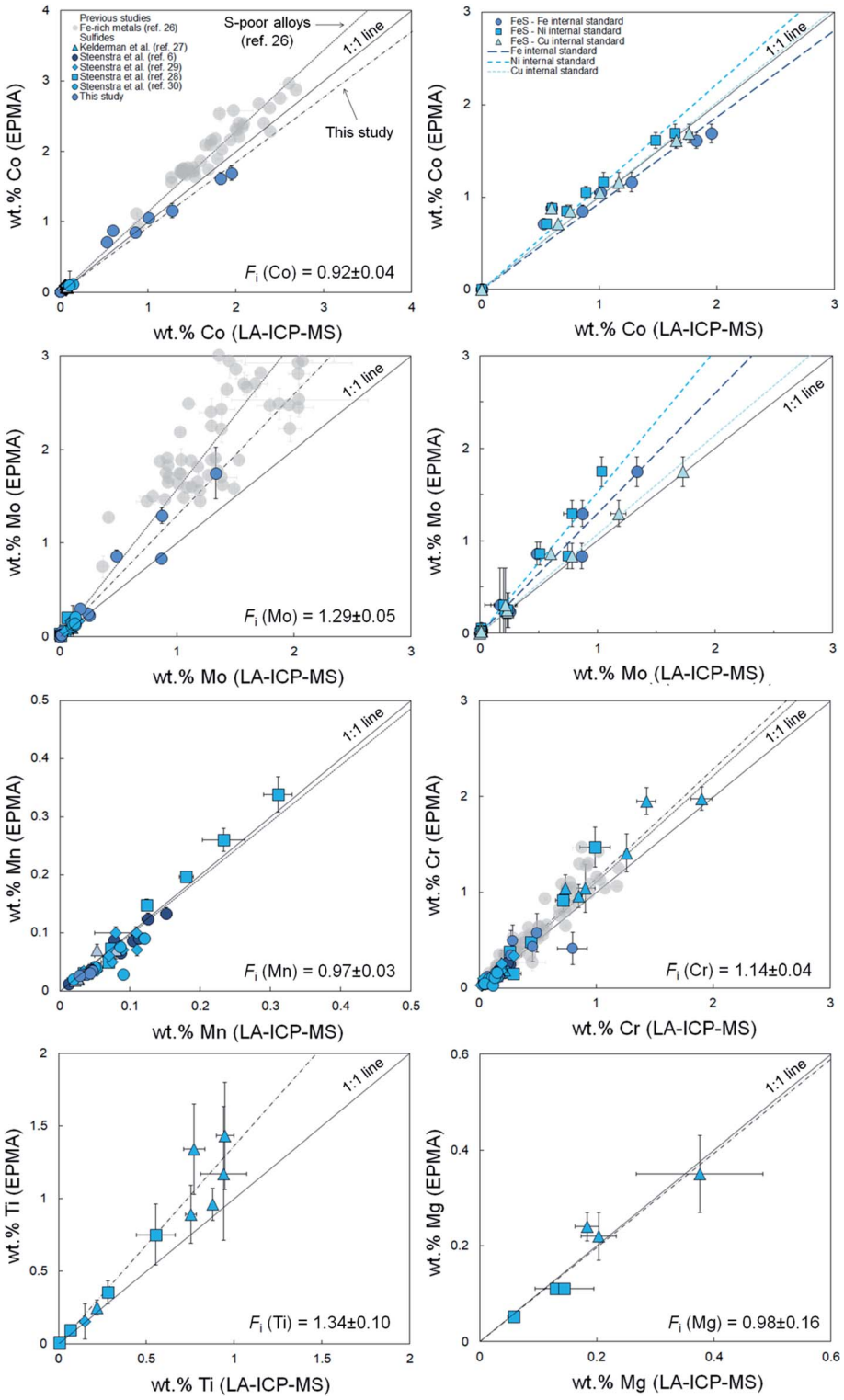

Fig. 4 Comparison between measured concentrations (%, in mass) of Co, Mo, Mn, Cr, Ti and Mg using LA-ICP-MS and EPMA for Fe-rich sulfides. See Fig. 1 caption for additional details.

an internal standard, with the F_i values obtained using Cu or Ni as an internal standard (Table 2 and right panels in Fig. 1–4, summarized in Fig. 6). For this purpose, only data from this study was considered, due to very low Ni and Cu concentrations in the sulfides from the previous studies, prohibiting the use of Ni or Cu as a reliable internal standard.[6,27–30] The F_i values for analyses that were calibrated using Ni as an internal standard are consistently higher than those obtained using Fe or Cu as an internal standard. This is especially evident from the much higher F_i values derived for

Table 2 Fractionation indices for Fe-rich sulfides assuming different internal standards. The F_i values were obtained using either measured EPMA and LA-ICP-MS concentrations for a set of samples (eqn (1)) or calculated using the F_i model derived in this study (eqn (2)). Listed for comparison are the F_i values derived for S-poor, Fe-rich metals of Steenstra *et al.*[26]

	50% cond. T (K)[34]	F_i (compiled, preferred), Fe internal standard[a]	N[b]	R^2[c]	Additional ref.[d]	F_i (this study only), Fe int. stand.[e]	N	R^2	F_i Ni int. stand.[f], Fe–S sulfide	N	R^2	F_i Cu int. stand.[g], Fe–S sulfide	N	R^2	F_i values Ni int. stand., S-poor metals[26]
Tl	532	0.64 ± 0.13[d]	—	—	—	—	—	—	—	—	—	—	—	—	0.29 ± 0.14
In	536	0.85 ± 0.04	16	0.99	—	0.85 ± 0.01	16	0.99	0.82 ± 0.04	16	0.97	0.71 ± 0.03	16	0.98	0.49 ± 0.03
Cd	652	0.66 ± 0.03	51	0.93	27–30	0.68 ± 0.04	16	0.95	0.61 ± 0.05	16	0.89	0.56 ± 0.04	16	0.90	0.14 ± 0.01
Se	697	1.34 ± 0.12[h]	67	0.91	6 and 27–30	1.78 ± 0.06	16	0.99	1.73 ± 0.16	16	0.89	1.72 ± 0.05	16	0.99	0.72 ± 0.04
Sn	704	0.73 ± 0.14	—	—	—	—	—	—	—	—	—	—	—	—	0.73 ± 0.07
Te	705	0.61 ± 0.09	58	0.84	6 and 27–30	0.71 ± 0.03	16	0.92	0.53 ± 0.07	16	0.79	0.71 ± 0.03	16	0.98	0.39 ± 0.03
Zn	726	0.86 ± 0.02[h]	52	0.97	27–30	1.00 ± 0.06	16	0.96	1.07 ± 0.08	16	0.93	1.01 ± 0.04	16	0.96	0.24 ± 0.06
Pb	727	0.72 ± 0.02	44	0.98	27–30	0.72 ± 0.02	16	0.99	0.78 ± 0.04	16	0.97	0.76 ± 0.02	16	0.99	0.35 ± 0.03
Bi	746	0.77 ± 0.05	41	0.86	27–30	0.81 ± 0.02	16	0.99	0.89 ± 0.05	16	0.96	0.82 ± 0.04	16	0.97	0.52 ± 0.17
Ge	883	0.72 ± 0.04	16	0.95	—	0.72 ± 0.04	16	0.95	0.67 ± 0.06	16	0.90	0.74 ± 0.04	16	0.96	1.09 ± 0.06
Ga	968	0.87 ± 0.16	—	—	—	—	—	—	—	—	—	—	—	—	0.77 ± 0.20
Sb	976	0.77 ± 0.02	16	0.99	—	0.77 ± 0.02	16	0.99	0.89 ± 0.04	16	0.98	0.59 ± 0.02	16	0.98	0.74 ± 0.04
Cu	1037	0.96 ± 0.03[h]	63	0.96	27–30	1.22 ± 0.06	16	0.97	1.42 ± 0.08	16	0.96	—	—	—	0.65 ± 0.03
As	1065	0.93 ± 0.03	16	0.99	—	0.93 ± 0.03	16	0.99	0.99 ± 0.04	16	0.98	0.93 ± 0.03	16	0.98	0.88 ± 0.04
Mn	1158	0.97 ± 0.03	44	0.94	27–30	—	—	—	—	—	—	—	—	—	—
P	1229	1.01 ± 0.18	—	—	—	—	—	—	—	—	—	—	—	—	0.82 ± 0.05
Cr	1296	1.14 ± 0.04	67	0.94	6 and 27–30	—	—	—	—	—	—	—	—	—	1.11 ± 0.03
Si	1302	1.05 ± 0.19	—	—	—	—	—	—	—	—	—	—	—	—	1.09 ± 0.02
Mg	1336	0.98 ± 0.16	6	0.90	27 and 28	—	—	—	—	—	—	—	—	—	—
Ni	1348	0.97 ± 0.02	56	0.97	27–30	0.97 ± 0.06	16	0.95	—	—	—	0.94 ± 0.06	16	0.94	0.95 ± 0.11
Co	1352	0.92 ± 0.04	21	0.97	30	0.93 ± 0.04	16	0.97	1.11 ± 0.03	16	0.99	1.01 ± 0.03	16	0.98	1.14 ± 0.06
Pt	1408	1.14 ± 0.04	18	0.98	6	—	—	—	—	—	—	—	—	—	—
V	1427	1.12 ± 0.20	—	—	—	—	—	—	—	—	—	—	—	—	1.39 ± 0.07
Nb	1559	1.19 ± 0.21	—	—	—	—	—	—	—	—	—	—	—	—	1.41 ± 0.28
Ta	1573	1.20 ± 0.21	—	—	—	—	—	—	—	—	—	—	—	—	1.42 ± 0.28
Ti	1582	1.34 ± 0.10	13	0.95	27 and 28	—	—	—	—	—	—	—	—	—	1.44 ± 0.28
Mo	1590	1.29 ± 0.05	38	0.95	27–30	1.30 ± 0.07	16	0.96	1.53 ± 0.08	16	0.96	1.07 ± 0.03	16	0.98	1.58 ± 0.10
U	1610	1.22 ± 0.21	—	—	—	—	—	—	—	—	—	—	—	—	1.47 ± 0.29
Th	1659	1.24 ± 0.21	—	—	—	—	—	—	—	—	—	—	—	—	1.52 ± 0.29
W	1789	1.31 ± 0.22	—	—	—	—	—	—	—	—	—	—	—	—	1.77 ± 0.15

[a] Fractionation indices in Fe–S sulfides for elements P, V, Ga, Si, Ti, Nb, Ta, Tl, U, Th, W were calculated using eqn (2). [b] Number of measurements included in regression. Regressions were based on data from this study and previous studies (ref. 6,27–30). [c] Coefficient of determination. [d] References used in addition to the experimental work presented in this study, obtained using a similar analytical approach.[6,27–30] [e] Fractionation indices calculated using Fe as an internal standard using only data from this study and includes zero count measurements for each sulfide. [f] Fractionation indices calculated using Ni as an internal standard using only data from this study and includes zero count measurements for each sulfide. [g] Fractionation indices calculated using Cu as an internal standard using only data from this study and includes zero count measurements for each sulfide. [h] Samples with high abundances of Se (>0.5 wt%), Zn (>3 wt%) and Cu (>1 wt%) were excluded due to significant F_i variations with increasing element concentrations.

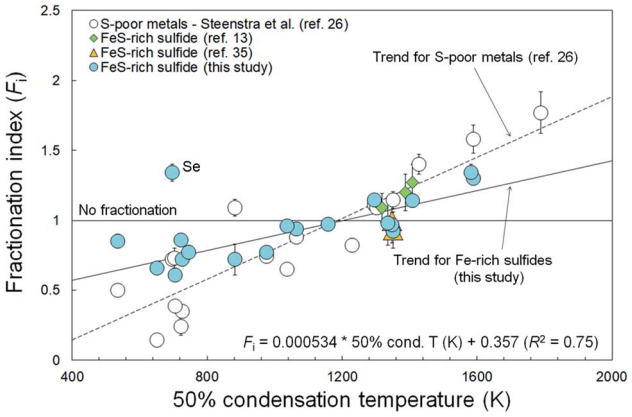

Fig. 5 Fractionation indices for sulfides from this study and ref. 13 and 35 as a function of their 50% condensation temperatures (based on the Ivuna carbonaceous chondritic composition at 10^{-4} bar (ref. 34)). Dashed line represents a linear fit to the calculated fractionation indices using F_i values from this study only. Previously derived F_i values for Fe-rich metal alloys from Steenstra *et al.* (ref. 26) and the corresponding relationship of F_i with volatility are plotted for comparison purposes.

Co, Cu, Sb and Mo (Fig. 4). The use of Ni therefore results in more pronounced matrix effects for refractory elements, but less so for volatile elements. The use of Cu as an internal standard results in F_i values that are on average lower than those derived for Fe, *i.e.*, increasing matrix effects for volatile elements, but decreasing them for refractory elements. These results show that the use of Ni is preferred for LA-ICP-MS of volatile elements in sulfides, whereas Cu is the preferred choice for refractory elements. If both types of elements are studied, Fe is recommended (Fig. 6).

4. Discussion

4.1 Comparison with previous work and differences between matrix effects for Fe-rich metals and Fe-rich sulfides for 193 nm ArF* laser systems

Wohlgemuth and Ueberwasser,[13] Halter *et al.*[35] and Sylvester[36] reported F_i values of Co, Ni, Cu, Zn and platinum group elements Pd, Rh and Pt for sulfides. The results for Co and Ni

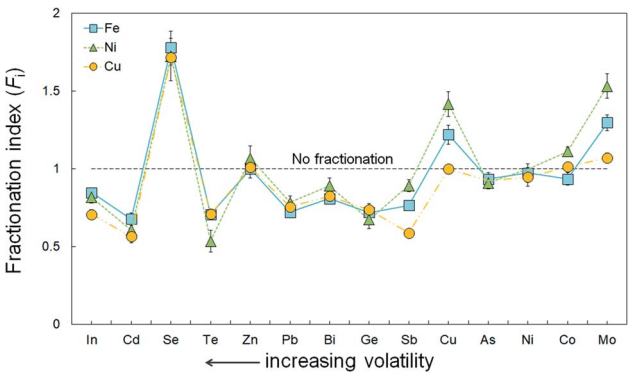

Fig. 6 Summary of F_i values for sulfides obtained using Fe, Ni or Cu as the internal standard for LA-ICP-MS analyses, plotted as a function of volatility (approximated here as the 50% condensation temperatures at 10^{-4} bar (ref. 34)).

obtained using a 193 nm ArF* laser system and the NIST 610 reference material (F_i (Co) = 0.93 ± 0.13; F_i (Ni) = 1.00 ± 0.10),[26,35,36] show no resolvable matrix effects – consistent with the results for both Fe-rich metals[26] and Fe-rich sulfides (this study) (Table 2). The lack of significant fractionation reported for Zn[13] for the 13 wt% Cu- and 21 wt% Zn bearing sulfide MASS-1 is consistent with the proposed decrease of the preferential ablation of Zn at higher Zn contents of the sulfide (Fig. 2) or, alternatively, could imply different ablation behavior of Zn in Cu-rich sulfides. The positive F_i values for Pt and Rh in sulfides obtained by ref. 13 (F_i (Rh) = 1.20 ± 0.13; F_i (Pt) = 1.27 ± 0.13) using a 193 ArF* laser system are consistent with the results obtained here and follow the proposed volatility trend of F_i for sulfides (Table 2 and Fig. 5).

Steenstra *et al.*[26] hypothesized – based on a limited number of F_i values for Fe-rich sulfides of elements that are classified as transitional to mildly refractory – that the magnitude of matrix effects for the elements of interest are similar for Fe-rich metals and Fe-rich sulfides. However, the results obtained in this study clearly show that the magnitude of matrix effects, both for refractory and volatile elements, are much smaller than those observed for Fe-rich metals.[26] The relative differences are approximately 45% for the most volatile and most refractory elements, respectively (Fig. 5). It is therefore concluded that matrix effect corrections derived for Fe-based samples cannot be applied to sulfides and that caution should be taken when extrapolating the new F_i values to Fe-poor sulfides (*e.g.*, NiS, ZnS, CuS).

There are several process(es) that could directly result in the specific matrix effects observed, such as differences in the vaporization of particles larger than 150 nm in the Ar plasma of the IPC or of fractional condensation of the cooling plume of the sample vapor between metals and sulfides. Our preferred explanation is that the pronounced differences between the matrix effects for Fe-rich metal samples and sulfides is due to the much more efficient ablation behavior of Fe-rich sulfides, and the corresponding decrease of the overall extent of non-congruent evaporation of more volatile elements from this melt.[36,37] Although the processes noted above, among others, may explain the general existence of volatility-related matrix effects, they do not directly account for differences *between* metal and sulfide matrices, whereas variable degrees of non-congruent evaporation does.

4.2 Implications for sulfide geochemistry

Due to the lack of suitable sulfide standards and/or matrix effect correction models and/or the low concentrations of many trace elements in sulfides, many studies of sulfide liquid – silicate melt partition coefficients ($D_i^{\text{sul liq–sil melt}}$, defined as the sulfide liquid to silicate melt abundance ratio of element i by weight)[5,6,24,27–30] and sulfide geochemistry (*e.g.*, ref. 23) relied solely on silicate primary standards for calibration of ns-LA-ICP-MS analyses of sulfides. The new results confirm that unresolved matrix effects during ns-LA-ICP-MS analyses of sulfides can strongly affect measured trace element concentrations[13,35,36] and therefore the experimentally determined $D_i^{\text{sul liq–sil melt}}$ values.

To illustrate the importance of the matrix effects, we computed the differences between uncorrected and corrected $D_i^{sul\ liq-sil\ melt}$ values for chalcophile ($\log D_i^{sul\ liq-sil\ melt} > 0$) and chalcophobic ($\log D_i^{sul\ liq-sil\ melt} < 0$) elements in Fig. 7. The necessity of incorporating matrix effects during ns-LA-ICP-MS analyses of sulfides by 193 nm ArF* laser systems while using non-matrix-matched standards is reflected by the differences between (un)corrected $D_i^{sul\ liq-sil\ melt}$ values for volatile- and refractory elements (Fig. 7). The differences between (un)corrected $D_i^{sul\ liq-sil\ melt}$ values are up to ~0.2 log units for the volatile elements (Cd, Se, Te, Tl) and up to ~0.15 log units for the most refractory elements (Ti, Mo, W). However, for most chalcophobic elements the uncertainties on $\log D^{sul\ liq-sil\ melt}{}_i$ values are similar or larger as the calculated offset due to the matrix effects (Fig. 7). For chalcophile elements the offset of $D_i^{sul\ liq-sil\ melt}$ values due to matrix effects are usually much larger than the corresponding analytical uncertainties on $\log D_i^{sul\ liq-sil\ melt}$ values.

Due to the contrasting matrix effects for Se and Te, relative differences between their (un)corrected $D_i^{sul\ liq-sil\ melt}$ values are up to ~0.35 log units. Given the geochemical significance of Se/Te ratios of sulfides, neglecting matrix effects would result in incorrect Se/Te ratios, thereby affecting corresponding geochemical models describing source region characteristics and magma evolution, such as those described in ref. 38. It should be noted that previous quantifications of the relative trace element partitioning behavior between sulfide liquids and monosulfide solid solution (MSS) (*e.g.*, ref. 38 and 39) are unlikely to have been affected by matrix effects, due to the similar chemical compositions of the latter phases.

As previously observed for S-poor metals,[7–12,26] failure to incorporate matrix effects on non-matrix-matched ns-LA-ICP-MS analyses of sulfides will result in significant inter-laboratory offsets of $D_i^{sul\ liq-sil\ melt}$ values and therefore introduces additional uncertainties in quantitative trace element geochemistry of sulfide phases.

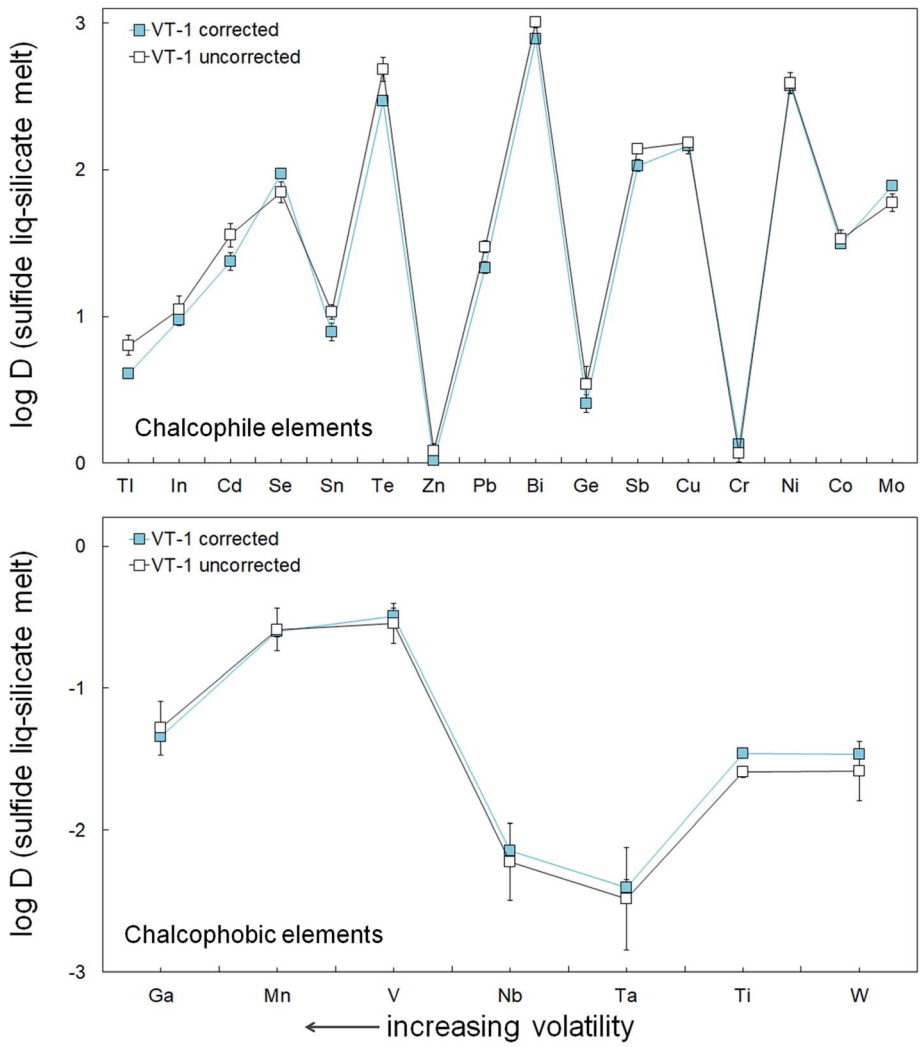

Fig. 7 Comparison between matrix-effect-corrected and uncorrected $D_i^{sul\ liq-sil\ melt}$ of run VT-1 (ref. 28) as a function of elemental volatility. Errors on $D_i^{sul\ liq-sil\ melt}$ values were calculated using simple error propagation, while assuming 2 standard errors on sulfide liquid and silicate melt concentrations of element i.

5. Conclusions

Elemental abundances in sulfides are commonly quantified by LA-ICP-MS using non-matrix-matched silicate primary standards, which could yield significant matrix effects. To address these matrix effects, individual fractionation indices (F_i values) were obtained for many elements for three different internal standards (Fe, Ni, Cu). It was found that F_i values for sulfides are significantly different than those derived for Fe-rich metal alloys. Nickel is the preferred internal standard for analysis of volatile elements, whereas Fe or Cu are recommended for the analysis of transitional and/or refractory elements. The results confirm the previously proposed importance of matrix effects arising from application of non-matrix-matched primary standards to measurements of elements in Fe-rich metals, brass samples and sulfides using LA-ICP-MS.

As previously observed for silicate glasses, brass targets and Fe-rich metal alloys, a good correlation is observed between elemental volatility and F_i values for sulfides. The correlation of F_i values with elemental volatility was used to obtain a new model for F_i that can be used to specifically predict F_i values for Fe-rich sulfides. Application of our results to sulfide geochemistry suggests that sulfide liquid–silicate melt partition coefficients may be under- and overestimated by up to 0.15 and 0.2 log units if matrix effects are not taken into account, respectively. Due to contrasting matrix effects for Se and Te, LA-ICP-MS derived Se/Te ratios of sulfides are even more strongly affected by matrix effects arising through the use of non-matrix-matched standards.

Conflicts of interest

There are no conflicts of interest to declare.

Acknowledgements

This work was supported financially by a Carnegie Fellow Postdoctoral Fellowship to E. S. S., a N. W. O. Vici grant to W. v. W. and by SFB grant TRR-170. We thank two anonymous reviewers for their constructive comments that improved the quality of the manuscript.

References

1 L. A. Vietti, J. V. Bailey, D. L. Fox and R. R. Rogers, *Palaios*, 2015, **30**(4), 327–334.
2 A. V. Andronikov, I. E. Andronikova and D. H. Hill, *Planet. Space Sci.*, 2015, **118**, 54–78.
3 N. J. Cook, C. L. Ciobanu and T. Williams, *Hydrometallurgy*, 2011, **108**, 226–228.
4 A. Luguet, J.-P. Lorand, O. Alard and J. Y. Cottin, *Chem. Geol.*, 2004, **208**, 175–194.
5 E. S. Kiseeva and B. J. Wood, *Earth Planet. Sci. Lett.*, 2015, **424**, 280–294.
6 E. S. Steenstra, A. X. Seegers, J. Eising, B. G. J. Tomassen, F. P. F. Webers, J. Berndt, S. Klemme, S. Matveev and W. van Westrenen, *Geochim. Cosmochim. Acta*, 2018, **231**, 130–156.
7 D. Bleiner, Z. Chen, D. Autrique and A. Bogaerts, *J. Anal. At. Spectrom.*, 2006, **21**, 910–921.
8 V. Možná, J. Pisonero, M. Holá, V. Kanický and D. Günther, *J. Anal. At. Spectrom.*, 2006, **21**(11), 1194–1201.
9 H.-R. Kuhn and D. Günther, *Anal. Chem.*, 2003, **75**, 747–753.
10 S. M. Chernonozhkin, S. Goderis, S. Bauters, B. Vekemans, L. Vincze, P. Claeys and F. Vanhaecke, *J. Anal. At. Spectrom.*, 2014, **29**, 1001–1016.
11 R. Glaus, R. Kaegi, F. Krumeich and D. Günther, *Spectrochim. Acta, Part B*, 2010, **65**, 812–822.
12 P. K. Diwakar, S. S. Harilal, N. L. LaHaye, A. Hassanein and P. Kulkarni, *J. Anal. At. Spectrom.*, 2013, **28**, 1420–1429.
13 C. C. Wohlgemuth-Ueberwasser and K. P. Jochum, *J. Anal. At. Spectrom.*, 2015, **30**, 2469–2480.
14 S. E. Gilbert, L. V. Danyushevsky, K. Goemann and D. Death, *J. Anal. At. Spectrom.*, 2014, **29**, 1024–1033.
15 L. Danyushevsky, P. Robinson, S. Gilbert, M. Norman, R. Large, P. McGoldrick and M. Shelley, *Geochem.: Explor., Environ., Anal.*, 2011, **11**, 51–60.
16 F. E. Jenner and H. S. C. O'Neill, *Geochem., Geophys., Geosyst.*, 2012, **13**, Q03003.
17 C. C. Wohlgemuth-Ueberwasser, C. Ballhaus, J. Berndt, V. Stotter nee Paliulionyte and T. Meisel, *Contrib. Mineral. Petrol.*, 2007, **154**, 607–617.
18 C. Ballhaus and P. Sylvester, *J. Petrol.*, 2001, **41**, 545–561.
19 L. J. Cabri, P. J. Sylvester, M. N. Tubrett, A. Peregoedova and L. H. G. Laflamme, *Can. Mineral.*, 2001, **41**, 321–329.
20 J. E. Mungall, D. R. A. Andrews, L. J. Cabri, P. J. Sylvester and M. Tubrett, *Geochim. Cosmochim. Acta*, 2005, **69**, 4349–4360.
21 J. Koch, S. Schlamp, T. Rosgen, D. Fliegel and D. Günther, *Spectrochim. Acta, Part B*, 2007, **62**, 20–29.
22 J. Koch and D. Günther, *Anal. Bioanal. Chem.*, 2007, **387**, 149–153.
23 B. Gourcerol, D. J. Kontak, P. C. Thurston and J. A. Petrus, *Miner. Deposita*, 2018, **53**, 871–894.
24 E. S. Kiseeva and B. J. Wood, *Earth Planet. Sci. Lett.*, 2013, **383**, 68–81.
25 A. T. Greaney, R. L. Rudnick, R. T. Helz, R. M. Gaschnig, P. M. Piccoli and R. D. Ash, *Geochim. Cosmochim. Acta*, 2017, **210**, 71–96.
26 E. S. Steenstra, J. Berndt, S. Klemme and W. van Westrenen, *J. Anal. Atomic Spectrom.*, 2019, **34**, 222–231.
27 E. K. Kelderman, E. S. Steenstra, J. Berndt, S. Klemme, A. Rohrbach and W. van Westrenen, *50th Lun. Planet. Sci. Conf., #1057 (abstr.)*, 2019.
28 E. S. Steenstra, V. T. Trautner, J. Berndt, S. Klemme and W. van Westrenen, *Icarus*, 2020, **335**, 113408.
29 E. S. Steenstra, J. Berndt, S. Klemme and W. van Westrenen, *50th Lun. Planet. Sci. Conf., #1137 (abstr.)*, 2019.
30 E. S. Steenstra, J. Berndt, S. Klemme, A. Rohrbach, E. S. Bullock and W. van Westrenen, *Geochim. Cosmochim. Acta*, 2020, **269**, 39–62.
31 J. T. Armstrong, *Microbeam Anal.*, 1995, **4**, 177–200.
32 T. Luo, Y. Wang, Z. C. Hu, D. Günther, Y. S. Liu, S. Gao, M. Li and S. H. Hu, *J. Anal. At. Spectrom.*, 2015, **30**, 941–949.

33 M. Gaboardi and M. Humayun, *J. Anal. At. Spectrom.*, 2009, **24**, 1188–1197.
34 K. Lodders, *Astrophys. J.*, 2003, **591**, 1220–1247.
35 W. E. Halter, T. Pettke and C. A. Heinrich, *Contrib. Mineral. Petrol.*, 2004, **147**, 385–396.
36 P. Sylvester, in *Laser Ablation-ICP-MS in the Earth Sciences, Current Practices and Outstanding Issues*, Mineralogical Association of Canada (MAC) Short Course Series, 2008, pp. 67–78.
37 R. Hergenröder, *J. Anal. Atomic Spectrom.*, 2006, 505–516.
38 J. M. Brenan, *Earth Planet. Sci. Lett.*, 2015, 45–57.
39 Y. Li and A. Audetat, *Earth Planet. Sci. Lett.*, 2012, **355–356**, 327–340.
40 W. L. Griffin, *Laser Ablation ICP-MS in the Earth Sciences: Current practices and outstanding issues*, 2008, pp. 308–311.